

Probe CP -violating $H\gamma\gamma$ coupling through interferometry

Xia Wan* and You-Kai Wang†

School of Physics & Information Technology, Shaanxi Normal University, Xi'an 710119, China

(Dated: December 2, 2021)

The diphoton invariant mass distribution of interference between $gg \rightarrow H \rightarrow \gamma\gamma$ and $gg \rightarrow \gamma\gamma$ is almost antisymmetric around the Higgs mass M_H . We propose a new observable A_{int} to quantify this effect, which is a ratio of a sign-reversed integral around M_H (e.g. $\int_{M_H-5}^{M_H} \text{GeV} - \int_{M_H}^{M_H+5} \text{GeV}$) and the cross section of the Higgs signal. We study A_{int} both in Standard Model (SM) and new physics with various CP -violating $H\gamma\gamma$ couplings. The A_{int} in SM could reach a value of 10%, while for CP -violating $H\gamma\gamma$ couplings A_{int} could range from 10% to -10% , which is probable to be detected in HL-LHC experiment. The A_{int} with both CP -violating $H\gamma\gamma$ and Hgg couplings are also studied and its value range is further extended.

I. INTRODUCTION

The CP violation, as one of the three Sakharov conditions [1], is necessary when explaining the matter-antimatter asymmetry in our universe [2]. Its source could have close relation with Higgs dynamics [3, 4]. Thus the CP properties of the 125 GeV Higgs boson with spin zero is proposed to be probed in various channels at the Large Hadron Collider (LHC) [5–24]. Among them, the golden channel $H \rightarrow ZZ \rightarrow 4\ell$ has been studied extensively and it gives relative stringent experimental constraints [19, 21, 22, 24]. By contrary, the $H \rightarrow \gamma\gamma$ process is another golden channel to discover Higgs boson and has a relative clean signature, but it suffers from lacking of CP -odd observable constructed from the self-conjugated diphoton signal kinematic variables. The CP property in $H\gamma\gamma$ coupling could also be studied in $H \rightarrow \gamma^*\gamma^* \rightarrow 4\ell$ process [25–27], however, it is challenged by the low conversion rate of the off-shell photon decaying into two leptons. In this paper, we study the CP property in $H\gamma\gamma$ coupling through the interference between $gg \rightarrow H \rightarrow \gamma\gamma$ and $gg \rightarrow \gamma\gamma$.

This interference has been studied in many papers [28–35]. Compared to the Breit-Wigner lineshape of the Higgs boson's signal, the lineshape of the interference term could be roughly divided into two parts: one is symmetric around M_H and the other is antisymmetric around M_H . These two kinds of interference lineshapes have different effects: after integrating over a symmetric mass region around M_H , the symmetric interference lineshape could reduce the signal Breit-Wigner cross section by $\sim 2\%$ [34]; while the antisymmetric one has no contribution to the total cross section, but could distort the signal lineshape, and shift the resonance mass peak by ~ 150 MeV [30, 33]. Besides, a variable A_i is proposed [36, 37] to quantify the interference effect in a sophisticated way, which defines a sign-reversed integral around M_H (e.g. $\int_{M_H-5}^{M_H} \text{GeV} dM - \int_{M_H}^{M_H+5} \text{GeV} dM$) in

its numerator and a sign-conserved integral around M_H (e.g. $\int_{M_H-5}^{M_H} \text{GeV} dM + \int_{M_H}^{M_H+5} \text{GeV} dM$) in its denominator, with both the integrands being overall lineshape, which is superimposed by the signal lineshape, the symmetric interference lineshape and the antisymmetric interference lineshape. In principal, all three effects from interference, changing signal cross section, shifting resonance mass peak and A_i (the ratio of sign-reversed integral and sign-conserved integral), could be used to probe CP violation in $H\gamma\gamma$ coupling, but their sensitivities are different. As the symmetric interference lineshape is contributed mainly from the Next-to-Leading order while the antisymmetric one from the leading order [29, 34], the effect from antisymmetric interference lineshape has better sensitivity, which means the latter two effects could be more sensitive to CP violation.

Nevertheless, experimentally A_i is not trivial, and could be affected a lot by the mass uncertainty of M_H [37]. The main reason is once M_H was deviated a little, the sign-reversed integral in the numerator would get a large extra value from the signal lineshape. To solve this problem, we suggest to separate the antisymmetric interference lineshape from the overall lineshape firstly, then replace the integrand in the numerator with only the antisymmetric interference lineshape. Thus the effect from the mass uncertainty is suppressed in the observable. The new modified observable is named as A_{int} and it is used to quantify the interference effect in our analysis.

In this paper, we study to probe the CP property in $H\gamma\gamma$ coupling through interference between $gg \rightarrow H \rightarrow \gamma\gamma$ and $gg \rightarrow \gamma\gamma$. The rest of the paper is organized as follows. In Section II, we introduce an effective model with a CP -violating $H\gamma\gamma$ coupling, and calculate the interference between $gg \rightarrow H \rightarrow \gamma\gamma$ and $gg \rightarrow \gamma\gamma$. Then we introduce the observable A_{int} , and study its dependence on CP violation. In Section III, we simulate the lineshapes of the signal and the interference, and get the A_{int} in SM and various CP -violation cases. After that, we estimate the feasibility to measure A_{int} at LHC and High Luminosity Large Hadron Collider (HL-LHC). In Section IV, we build a general framework with both CP violating $H\gamma\gamma$ and Hgg couplings and study the A_{int} in a same

* wanxia@snnu.edu.cn

† wangyk@snnu.edu.cn

procedure as above. In Section V, we give a conclusion and discussion.

II. THEORETICAL CALCULATION

The effective model with a CP -violating $H\gamma\gamma$ coupling is given as,

$$\mathcal{L}_h = \frac{c_\gamma \cos \xi_\gamma}{v} h F_{\mu\nu} F^{\mu\nu} + \frac{c_\gamma \sin \xi_\gamma}{2v} h F_{\mu\nu} \tilde{F}^{\mu\nu} + \frac{c_g}{v} h G_{\mu\nu}^a G^{a\mu\nu}, \quad (1)$$

where F , G^a denote the γ and gluon field strengths, $a = 1, \dots, 8$ are $SU(3)_c$ adjoint representation indices for the gluons, $v = 246$ GeV is the electroweak vacuum expectation value, the dual field strength is defined as $\tilde{X}^{\mu\nu} = \epsilon^{\mu\nu\sigma\rho} X_{\sigma\rho}$, c_γ and c_g are effective couplings in SM at leading order, $\xi_\gamma \in [0, 2\pi)$ is a phase that parametrize CP violation. When $\xi_\gamma = 0$, it is the SM case; when $\xi_\gamma \neq 0$, there must exist CP violation (except for $\xi_\gamma = \pi$) and new physics beyond SM. This kind of parametrization could make sure that the total signal strength of Higgs decaying to diphoton is equal to one as predicted by SM.

In SM at leading order, c_γ is introduced by fermion and W loops and c_g is introduced by fermion loops only, which have the expressions as

$$c_g = \frac{\alpha_s}{16\pi} \sum_{f=t,b} F_{1/2}(4m_f^2/\hat{s}), \quad (2)$$

$$c_\gamma = \frac{\alpha}{8\pi} \left[F_1(4m_W^2/\hat{s}) + \sum_{f=t,b} N_c Q_f^2 F_{1/2}(4m_f^2/\hat{s}) \right] \quad (3)$$

where $\alpha_s(\alpha)$ are running QCD(QED) couplings, $N_c = 3$, Q_f and m_f are electric charge and mass of fermions, and

$$F_{1/2}(\tau) = -2\tau[1 + (1 - \tau)f(\tau)], \quad (4)$$

$$F_1(\tau) = 2 + 3\tau[1 + (2 - \tau)f(\tau)], \quad (5)$$

$$f(\tau) = \begin{cases} \arcsin^2 \sqrt{1/\tau} & \tau \geq 1, \\ -\frac{1}{4} \left[\log \frac{1+\sqrt{1-\tau}}{1-\sqrt{1-\tau}} - i\pi \right]^2 & \tau < 1. \end{cases} \quad (6)$$

The helicity amplitudes for $gg \rightarrow H \rightarrow \gamma\gamma$ and $gg \rightarrow \gamma\gamma$ can be written as [30, 38, 39],

$$\mathcal{M} = -e^{-ih_3\xi_\gamma} \delta^{h_1 h_2} \delta^{h_3 h_4} \delta^{ab} \frac{M_{\gamma\gamma}^4}{v^2} \frac{4c_g c_\gamma}{M_{\gamma\gamma}^2 - M_H^2 + iM_H \Gamma_H} + 4\alpha_s \delta^{ab} \sum_{f=u,d,c,s,b} Q_f^2 \mathcal{A}_{\text{box}}^{h_1 h_2 h_3 h_4}, \quad (7)$$

where a, b are the same as a in Eq. (1), the spinor phases (see their concrete formulas in [38, 39] and [16]) are dropped for simplicity, h_i s are helicities of outgoing gluons and photons, Q_f is the electric charge of

fermion, $\mathcal{A}_{\text{box}}^{h_1 h_2 h_3 h_4}$ are reduced 1-loop helicity amplitudes of $gg \rightarrow \gamma\gamma$ mediated by five flavor quarks, while the contribution from top quark is much suppressed [28] and is neglected in our analysis. The \mathcal{A}_{box} for non-zero interference are [30, 38, 39]

$$\begin{aligned} \mathcal{A}_{\text{box}}^{++++} &= \mathcal{A}_{\text{box}}^{----} = 1, \\ \mathcal{A}_{\text{box}}^{++--} &= \mathcal{A}_{\text{box}}^{--++} = \\ &-1 + z \ln \left(\frac{1+z}{1-z} \right) - \frac{1+z^2}{4} \left[\ln^2 \left(\frac{1+z}{1-z} \right) + \pi^2 \right], \end{aligned} \quad (8)$$

where $z = \cos \theta$, with θ being the scattering angle of γ in diphoton center of mass frame. It maybe noticed by a careful reader that we use the formulas for $\mathcal{A}_{\text{box}}^{++++/-}$ and $\mathcal{A}_{\text{box}}^{++--/-}$ as same as in [38, 39], which are swapped in [30]. That is because the convention we used here are for outgoing gluons, the helicities would be changed to a reversed sign if for incoming gluons. It is also worthwhile to notice that Eq. (7) is different from Eq. (2) in Ref. [30] because of the $e^{-ih_3\xi_\gamma}$ factor, which determines that the Higgs signal strength are not affected by the CP -violation factor ξ_γ , but the interference strength has a simple $\cos \xi_\gamma$ dependence (see Eqs. (9)(10)).

After considering interference, the lineshape over the smooth background is composed of both lineshapes of signal and interference, which can be expressed by

$$\begin{aligned} \frac{d\sigma_{\text{sig}}}{dM_{\gamma\gamma}} &= \frac{G(M_{\gamma\gamma})}{128\pi M_{\gamma\gamma}} \frac{|c_g c_\gamma|^2}{(M_{\gamma\gamma}^2 - M_H^2)^2 + M_H^2 \Gamma_H^2} \times \int dz, \quad (9) \\ \frac{d\sigma_{\text{int}}}{dM_{\gamma\gamma}} &= \frac{G(M_{\gamma\gamma})}{128\pi M_{\gamma\gamma}} \frac{(M_{\gamma\gamma}^2 - M_H^2) \text{Re}(c_g c_\gamma) + M_H \Gamma_H \text{Im}(c_g c_\gamma)}{(M_{\gamma\gamma}^2 - M_H^2)^2 + M_H^2 \Gamma_H^2} \\ &\times \int dz [\mathcal{A}_{\text{box}}^{++++} + \mathcal{A}_{\text{box}}^{++--}] \times \cos \xi_\gamma, \end{aligned} \quad (10)$$

where $\sigma_{\text{sig}}, \sigma_{\text{int}}$ are cross sections from signal term and interference term respectively, $M_{\gamma\gamma} = \sqrt{\hat{s}}$, the integral region of z depends on the detector angle coverage in experiment, $G(M_{\gamma\gamma})$ is gluon-gluon luminosity function written as

$$G(M_{\gamma\gamma}) = \int_{M_{\gamma\gamma}^2/s}^1 \frac{dx}{sx} [g(x)g(M_{\gamma\gamma}^2/(sx))]. \quad (11)$$

The interference term consists of two parts: antisymmetric (the first term in Eq. (10)) and symmetric (the second term in Eq. (10)) parts around Higgs boson's mass. It is worthy to notice that at leading order $\text{Im}(c_g^{\text{SM}} c_\gamma^{\text{SM}})$ is suppressed by m_b/m_t compared to $\text{Re}(c_g^{\text{SM}} c_\gamma^{\text{SM}})$ because the imaginary parts of $c_g^{\text{SM}}, c_\gamma^{\text{SM}}$ are mainly from bottom quark loop while their real parts are from top quark or W boson loop. Thus the symmetric part of the interference term is much suppressed at leading order and its integral value contributed for the total cross section is mainly from Next-to-Leading order [28, 34]. By contrast, the antisymmetric part could have a larger magnitude around M_H .

The observable A_{int} extracts the antisymmetric part of the interference by an sign-reversed integral around M_H , which is defined as

$$A_{\text{int}}(\xi_\gamma) = \frac{\int dM_{\gamma\gamma} \frac{d\sigma_{\text{int}}}{dM_{\gamma\gamma}} \Theta(M_{\gamma\gamma} - M_H)}{\int dM_{\gamma\gamma} \frac{d\sigma_{\text{sig}}}{dM_{\gamma\gamma}}}, \quad (12)$$

where the integral region is around Higgs resonance (e.g. [121, 131] GeV for $M_H = 126$ GeV), the Θ -function is

$$\Theta(x) \equiv \begin{cases} -1, & x < 0 \\ 1, & x > 0 \end{cases}.$$

So the numerator keeps the antisymmetric contribution from the interference, and the denominator is the cross section from the signal, A_{int} is an observable that roughly indicates the ratio of the interference to the signal.

As $\xi_\gamma = 0$ represents the SM case, we could define $A_{\text{int}}^{\text{SM}} \equiv A_{\text{int}}(\xi_\gamma = 0)$ and rewrite $A_{\text{int}}(\xi_\gamma)$ simply as

$$A_{\text{int}}(\xi_\gamma) = A_{\text{int}}^{\text{SM}} \times \cos \xi_\gamma. \quad (13)$$

The largest deviation $A_{\text{int}}(\pi) = -A_{\text{int}}^{\text{SM}}$ happens when $\xi_\gamma = \pi$, which represents an inverse CP-even $H\gamma\gamma$ coupling from new physics but without CP violation. It's interesting that this degenerate coupling could only be exhibited by the interference effect.

III. NUMERICAL RESULTS

The numerical results are obtained for proton-proton collision with $\sqrt{s} = 14$ TeV by using the MCFM [40] package, in which the subroutines according to the helicity amplitudes of Eq. (7) are added. The Higgs boson's mass and width are set as $M_H = 126$ GeV, and $\Gamma_H = 4.3$ MeV. Each photon is required to have $p_T^\gamma > 20$ GeV and $|\eta^\gamma| < 2.5$. Based on the simulation, we study $A_{\text{int}}^{\text{SM}}$ firstly and then A_{int} from CP violation cases. After that, we estimate the feasibility to extract A_{int} out at LHC.

A. $A_{\text{int}}^{\text{SM}}$

Fig. 1 show the theoretical lineshapes of the signal (a sharp peak shown in the black histogram) and the interference (a peak and dig shown in the red histogram), among which Fig. 1a is an overall plot, Fig. 1b and Fig. 1c are close-ups. As shown in Fig. 1a and Fig. 1b, the signal has a mass peak that is about four times of the interference, but the mass peak of the interference is wider and has a much longer tail. The resonance region [125.9, 126.1] GeV is further scrutinized in Fig. 1c with bin width changed from 100 MeV to 2 MeV. The value of the signal exceeds that of the interference at the energy point $M_{\gamma\gamma} \approx M_H - 10 \times \Gamma_H$. After integrating, the $A_{\text{int}}^{\text{SM}}$

TABLE I. The $A_{\text{int}}^{\text{SM}}$ values with different mass resolution widths. The $\sigma_{\text{MR}} = 0$ represents the theoretical case before Gaussian smearing.

σ_{MR} (GeV)	$A_{\text{int}}^{\text{SM}}$ denominator (fb)	$A_{\text{int}}^{\text{SM}}$ numerator (fb)	$A_{\text{int}}^{\text{SM}}$ (%)
0	39.3	14.3	36.3
1.1	39.3	4.0	10.2
1.3	39.3	3.7	9.4
1.5	39.3	3.4	8.6
1.7	39.3	3.1	7.9
1.9	39.3	2.8	7.2

is 36% as shown in table I, which is quite large. As the smearing by the mass resolution (MR) is not considered yet, we mark it as the $\sigma_{\text{MR}} = 0$ case.

The invariant mass of the diphoton $M_{\gamma\gamma}$ has a mass resolution of about 1 ~ 2 GeV at the LHC experiment [41]. For simplicity we include the mass resolution effect by convoluting the histograms with a Gaussian function of width $\sigma_{\text{MR}} = 1.1, 1.3, 1.5, 1.7, 1.9$ GeV. This convolution procedure is also called Gaussian smearing. Fig. 2 shows the lineshapes after the Gaussian smearing with $\sigma_{\text{MR}} = 1.5$ GeV. The sharp peak of the signal becomes a wide bump (the black histogram), meanwhile, the peak and dig of the interference are also widened, but they cancel each other a lot near M_H and the former peak and dig becomes a moderate antisymmetric shape around M_H . (the red histogram). The $A_{\text{int}}^{\text{SM}}$ after Gaussian smearing is thus much reduced, which range from 10.2% to 7.2% when σ_{MR} goes from 1.1 to 1.9 GeV as shown in table I.

B. $A_{\text{int}}(\xi_\gamma \neq 0)$

Fig. 3 shows the lineshapes of interference under the $\xi_\gamma = 0, \pi, \pi/2$ cases with $\sigma_{\text{MR}} = 1.5$ GeV. The blue histogram ($\xi_\gamma = \pi$, sign-reversed CP-even $H\gamma\gamma$ coupling) is almost opposite to the red histogram ($\xi_\gamma = 0$, SM), which correspond to the minimum and the maximum of A_{int} values. The black dashed histogram ($\xi_\gamma = \pi/2$, CP-odd $H\gamma\gamma$ coupling) looks like a flat line (actually with some tiny fluctuation from simulation), and it corresponds to zero A_{int} value. Fig. 4 shows A_{int} and its absolute statistical error δA_{int} . The statistical error is estimated with an integrated luminosity of 30 fb⁻¹, and the efficiency of detector is assumed to be one. δA_{int} decrease as A_{int} becomes smaller, however, the relative statistical error $\delta A_{\text{int}}/A_{\text{int}}$ increase quickly and becomes very large as A_{int} approaches zero. In SM ($\xi_\gamma = 0$ in Fig. 4), the relative statistical error $\delta A_{\text{int}}/A_{\text{int}}$ is about 18% with an assumption of zero correlation between symmetric and antisymmetric cross-sections.

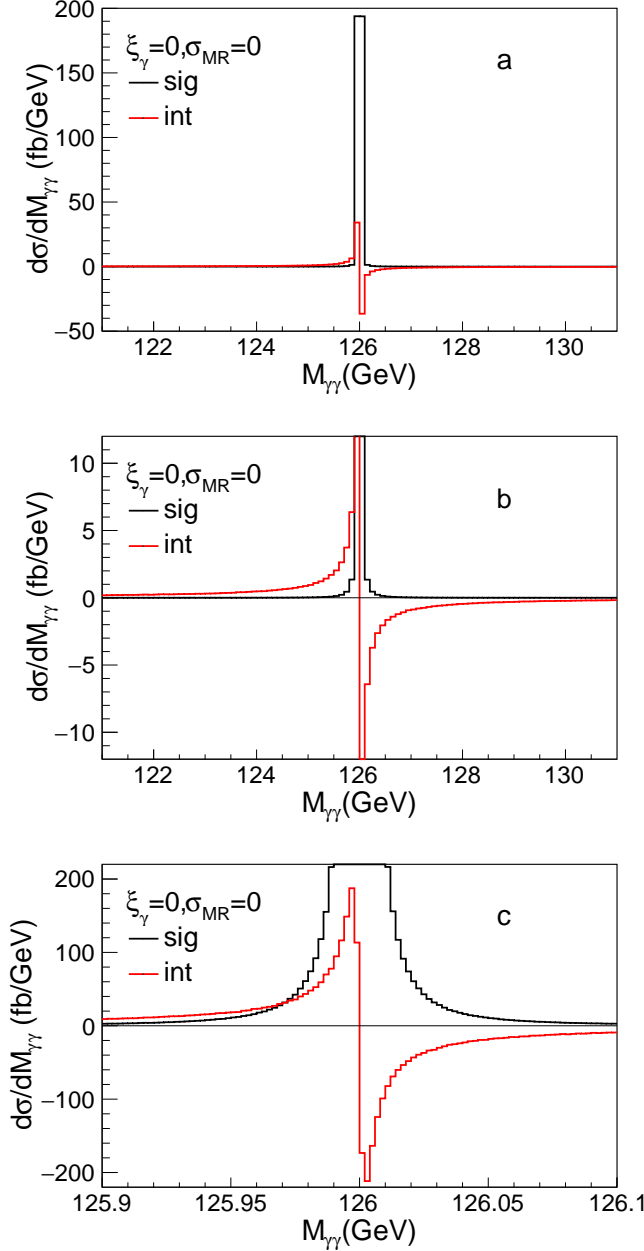


FIG. 1. The diphoton invariant mass $M_{\gamma\gamma}$ distribution of the signal and the interference as in Eq. (9) and (10). $\xi_\gamma = 0$ represents the SM case, $\sigma_{\text{MR}} = 0$ represents the theoretical distribution before Gaussian smearing. Among them (a) is an overall plot, (b) and (c) are close-ups.

C. A_{int} at LHC

In current CMS or ATLAS experiment, the $\gamma\gamma$ mass spectrum is fitted by a signal function and a background function. To consider the interference effect, the anti-symmetric lineshape should also be included. That is, instead of a Gaussian function (or a double-sided Crystal

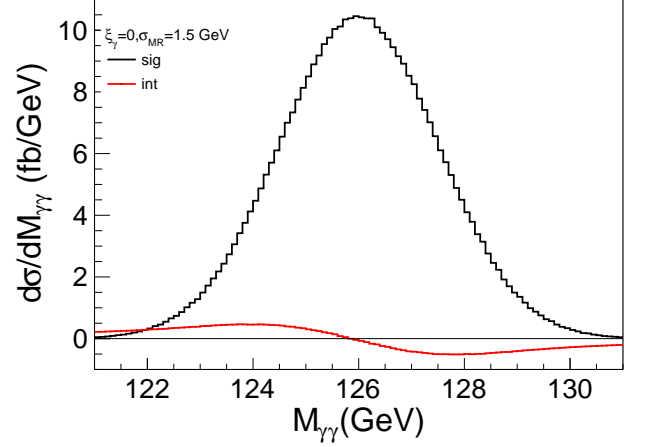


FIG. 2. The diphoton invariant mass $M_{\gamma\gamma}$ distribution after Gaussian smearing with its mass resolution width $\sigma_{\text{MR}} = 1.5$ GeV.

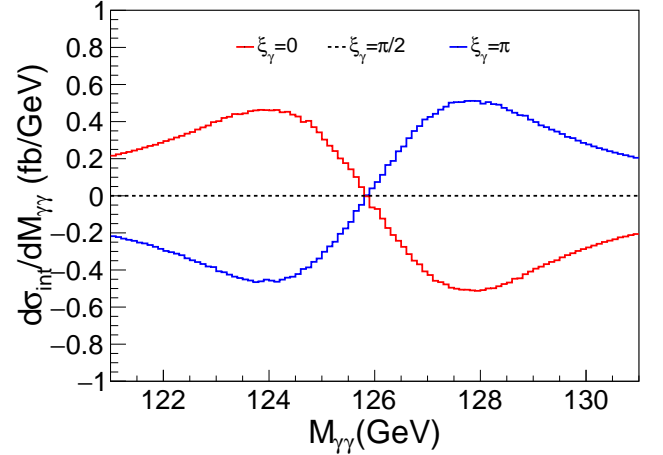


FIG. 3. The diphoton invariant mass $M_{\gamma\gamma}$ distribution of interference after Gaussian smearing with $\sigma_{\text{MR}} = 1.5$ GeV when $\xi_\gamma = 0, \pi, \pi/2$.

tal Ball function) as the signal function in current LHC experiment [41, 42], a Gaussian function (or a double-sided Crystal Ball function) plus an asymmetric function should be used as the modified signal function, while the background function is kept as same as in the experiment.

To see whether or not the asymmetric lineshape could be extracted, we carry out a modified-signal fitting on two background-subtracted data samples. As the background fluctuation would be dealt with similarly as in real experiment, we ignore it here for simplicity. One data sample is from the CMS experiment in Ref. [41], we fetch 10 data points with its errors between [121, 131] GeV in the background-subtracted $\gamma\gamma$ mass spectrum for 35.9 fb^{-1} luminosity with proton-proton

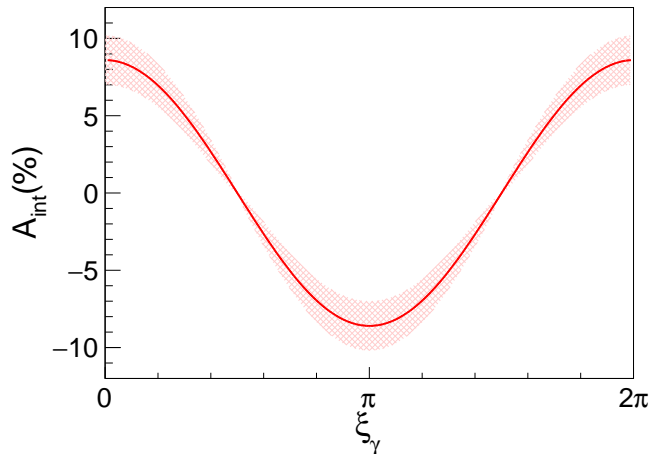


FIG. 4. A_{int} values (red line) and its statistical error (shade) with different phase ξ_γ .

collide energy at 13 TeV (see Fig. 13 in Ref. [41]). The fitting function is described as

$$f(m) = c_1 \times f_{\text{sig}}(m - \delta m) + c_2 \times f_{\text{int}}(m - \delta m), \quad (14)$$

where $c_1, c_2, \delta m$ are float parameters, m means the value of the $\gamma\gamma$ invariant mass, the functions $f_{\text{sig}}(m), f_{\text{int}}(m)$ are evaluated from the two histograms in Fig. 2 and they describe the signal and interference separately. Fig. 5 shows the fitting result on the CMS data, in which the crosses represent CMS data with its error, the red solid line is the combined function, the black dashed line and the blue dotted line represent the signal and interference components respectively. The black dashed line is almost same as the red solid line while the blue dotted line is almost flat, the fitting parameter c_2 for the interference component has a huge uncertainty that is even larger than the central value of c_1 , which indicates the interference component is hard to be extracted from the 35.9 fb^{-1} CMS data. For a comparison, we simulate a pseudodata sample from the combined histogram in Fig. 2, which is normalized to have events of about 80 times the CMS data (corresponding to a luminosity of 3000 fb^{-1}), with a binwidth of 0.5 GeV and Poisson fluctuation. The fitting result is shown in Fig. 6, where the red solid line has a shift from the black dashed line, the blue dotted line could be distinguishable clearly. c_1 and c_2 are fitted as $c_1 = 0.999 \pm 0.002$, $c_2 = 0.947 \pm 0.028$, which are consistent with their SM expected value 1 and deduce to a relative error of $A_{\text{int}} \sim 3\%$ according to the error propagation formula. Even though this fitting result looks quite good, it can only reflect that the antisymmetric lineshape could be extracted out when no contamination comes from systematic error. Furthermore, our study shows that the optimal fitting strategy is taking Higgs mass as a free parameter together with c_1 and c_2 . Although M_H has been measured in many channels, its

fluctuation is usually too large to get a converged fitting if we take it as a known input value.

By contrast, a simulation that also study the interference effect has been carried out with systematic error included by ATLAS collaboration at HL-LHC with a luminosity of 3000 fb^{-1} [43]. In that simulation, the mass shift of Higgs boson caused by the interference effect has been studied under different Higgs' width assumptions. A pseudo-data is produced by smearing a Breit-Wigner with the resolution model and the interference effect are described by the shift of smeared Breit-Wigner distributions. Based on fitting, the mass shift of Higgs from the interference effect is estimated to be $\Delta m_H = -54.4 \text{ MeV}$ for the SM case, and the systematic error on the mass difference is about 100 MeV. If using this result to estimate the mass shift effect for the non-SM $\xi_\gamma \neq 0$ cases, that would be, $\xi_\gamma = \pi/2$ corresponds to a zero mass shift, and $\xi_\gamma = \pi$ corresponds to a reverse mass shift of $\Delta m_H = +54.4 \text{ MeV}$ as shown in Fig. 3. Then the largest deviation of the mass shift from the SM case is $2 \times 54.4 \text{ MeV}$ (when $\xi_\gamma = \pi$), which is almost covered by the systematic error of 100 MeV. Therefore, the non-SM $\xi_\gamma \neq 0$ cases could not be distinguished through this mass shift effect. Nevertheless, it is worthing to note that the antisymmetric lineshape of the interference effect by theoretical calculation is quite different from the shift of two smeared Breit-Wigner distributions in ATLAS's simulation [43], especially at the region far from the Higgs' peak, the antisymmetric lineshape of the interference effect has a longer flat tail while the Breit-Wigner distribution falls fast. The authors from ATLAS collaboration has also noticed this difference and planned to add it to their next research [43].

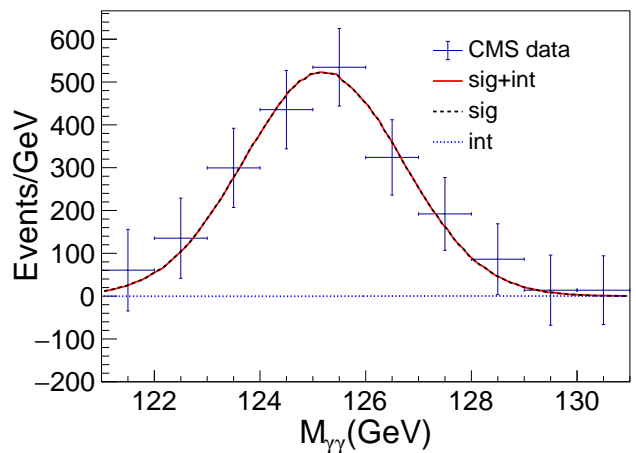


FIG. 5. A fitting on the background-subtracted CMS data sample. The crosses represent CMS data from Ref. [41]. The red solid line is the combined function, the black dashed line and the blue dotted line represent the signal and interference components respectively.

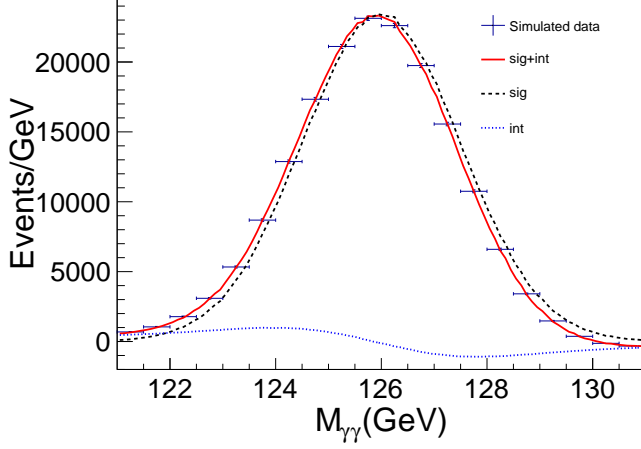


FIG. 6. A fitting on the simulated data sample. The crosses represent simulated data from the combined histogram in Fig. 2 normalized to a luminosity of 3000 fb^{-1} . The red solid line is the combined function, the black dashed line and the blue dotted line represent the signal and interference components respectively.

IV. CP VIOLATION IN Hgg COUPLING

In the above study the Hgg coupling is supposed to be SM-like, furthermore, the observable A_{int} could also be used to probe CP violation in Hgg coupling. In this section, we add one more parameter ξ_g to describe CP violation in Hgg coupling, and study A_{int} following the same procedure as above.

Based on Eq. (1), one more parameter ξ_g to describe CP violation in Hgg coupling is added, and the effective Lagrangian is modified as

$$\mathcal{L}_h = \frac{c_\gamma \cos \xi_\gamma}{v} h F_{\mu\nu} F^{\mu\nu} + \frac{c_\gamma \sin \xi_\gamma}{2v} h F_{\mu\nu} \tilde{F}^{\mu\nu} + \frac{c_g \cos \xi_g}{v} h G_{\mu\nu}^a G^{a\mu\nu} + \frac{c_g \sin \xi_g}{2v} h G_{\mu\nu}^a \tilde{G}^{a\mu\nu} \quad (15)$$

After that, the helicity amplitude in Eq. (7) and differential cross section of interference in Eq. (10) should be changed correspondingly, which are

$$\mathcal{M} = -e^{-ih_1\xi_g} e^{-ih_3\xi_\gamma} \delta^{h_1 h_2} \delta^{h_3 h_4} \delta^{ab} \frac{M_{\gamma\gamma}^4}{v^2} \frac{4c_g c_\gamma}{M_{\gamma\gamma}^2 - M_H^2 + iM_H \Gamma_H} + 4\alpha\alpha_s \delta^{ab} \sum_{f=u,d,c,s,b} Q_f^2 \mathcal{A}_{\text{box}}^{h_1 h_2 h_3 h_4}, \quad (16)$$

$$\frac{d\sigma_{\text{int}}}{dM_{\gamma\gamma}} \propto \frac{(M_{\gamma\gamma}^2 - M_H^2) \text{Re}(c_g c_\gamma) + M_H \Gamma_H \text{Im}(c_g c_\gamma)}{(M_{\gamma\gamma}^2 - M_H^2)^2 + M_H^2 \Gamma_H^2} \times \int dz [\cos(\xi_g + \xi_\gamma) \mathcal{A}_{\text{box}}^{++++} + \cos(\xi_g - \xi_\gamma) \mathcal{A}_{\text{box}}^{++--}] \quad (17)$$

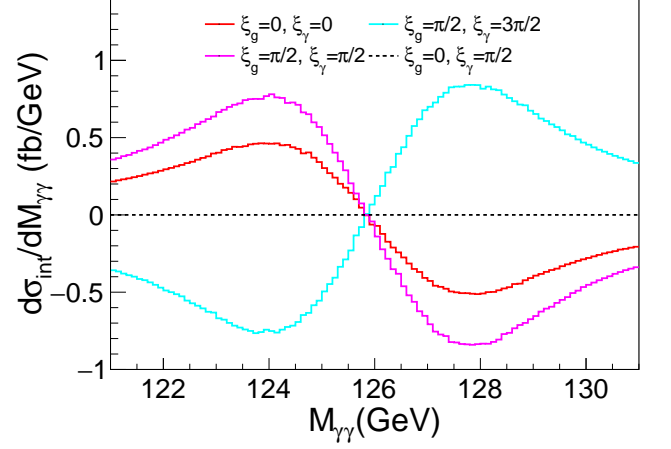


FIG. 7. The diphoton invariant mass $M_{\gamma\gamma}$ distribution of interference after Gaussian smearing in various ξ_g , ξ_γ cases.

Then $A_{\text{int}}^{\text{SM}} \equiv A_{\text{int}}(\xi_g = 0, \xi_\gamma = 0)$ and

$$A_{\text{int}}(\xi_g, \xi_\gamma) = A_{\text{int}}^{\text{SM}} \times \frac{\int dz [\cos(\xi_g + \xi_\gamma) \mathcal{A}_{\text{box}}^{++++} + \cos(\xi_g - \xi_\gamma) \mathcal{A}_{\text{box}}^{++--}]}{\int dz [\mathcal{A}_{\text{box}}^{++++} + \mathcal{A}_{\text{box}}^{++--}]} \quad (18)$$

where the integral could be calculated numerically once the the integral region of z is given. For example, if the pseudorapidity of γ is required to be $|\eta^\gamma| < 2.5$, that is, $z \in [-0.985, 0.985]$, the integral $\int dz \mathcal{A}_{\text{box}}^{++--} \approx -9$, and Eq. (18) could be simplified as

$$A_{\text{int}}(\xi_g, \xi_\gamma) \approx A_{\text{int}}^{\text{SM}} \times \frac{2 \cos(\xi_g + \xi_\gamma) - 9 \cos(\xi_g - \xi_\gamma)}{-7}. \quad (19)$$

$A_{\text{int}}(\xi_g, \xi_\gamma)$ thus has a maximum and minimum of about 1.6 times of $A_{\text{int}}^{\text{SM}}$. If $\xi_g = 0$, $A_{\text{int}}(\xi_g = 0, \xi_\gamma)$ will degenerate to the $A_{\text{int}}(\xi_\gamma)$ in Eq. (13). By contrast, if $\xi_\gamma = 0$,

$$A_{\text{int}}(\xi_g) = A_{\text{int}}^{\text{SM}} \times \cos(\xi_g), \quad (20)$$

which shows the same dependence of $A_{\text{int}}(\xi_\gamma)$ on ξ_γ when $\xi_g = 0$ as in Eq. (13). So a CP -violating Hgg coupling could cause similar deviation of A_{int} to $A_{\text{int}}^{\text{SM}}$ as a CP -violating $H\gamma\gamma$ coupling, and an single observed A_{int} value could not distinguish them since there are two free parameters for one observable.

Fig. 7 shows the lineshapes of interference for different ξ_g , ξ_γ choices. The red histogram ($\xi_g = 0$, $\xi_\gamma = 0$) represents the SM case; the magenta histogram ($\xi_g = \frac{\pi}{2}$, $\xi_\gamma = \frac{\pi}{2}$) could get largest A_{int} ; the cyan histogram ($\xi_g = \frac{\pi}{2}$, $\xi_\gamma = \frac{3\pi}{2}$) corresponds to the smallest A_{int} ; and the black histogram is from $\xi_g = 0$, $\xi_\gamma = \frac{\pi}{2}$ case with A_{int} equal to zero. For the general case of both ξ_g , ξ_γ being free parameters, $A_{\text{int}}(\xi_g, \xi_\gamma)$ could have a wider value range than $A_{\text{int}}(\xi_\gamma)$, which makes it easier to be probed in future experiment.

V. CONCLUSION AND DISCUSSION

The diphoton mass distribution from the interference between $gg \rightarrow H \rightarrow \gamma\gamma$ and $gg \rightarrow \gamma\gamma$ at leading order is almost antisymmetric around M_H and we propose an sign-reversed integral around M_H to get its contribution. After dividing this integral value by the cross section of Higgs signal, we get an observable A_{int} . In SM, the theoretical A_{int} value before taking into account the mass resolution could be $\sim 39\%$. After considering mass resolution of ~ 1.5 GeV, A_{int} is reduced but still could be as large as 10% . The CP violation in $H\gamma\gamma$ could change A_{int} from 10% to -10% depending on the CP violation phase ξ_γ . In a general framework of both CP -violating $H\gamma\gamma$ and Hgg coupling, A_{int} could have a larger value

of $\sim \pm 16\%$. However, due to the systematic error and statistical error are both $\sim 10\%$ in current experiments at LHC, the antisymmetric lineshape is difficult to be extracted out. Even at futuristic high luminosities, the large systematic error is still a tricky obstacle.

ACKNOWLEDGMENTS

The work is supported by the National Natural Science Foundation of China under Grant No.11405102 and No.11847168, and the Fundamental Research Funds for the Central Universities of China under Grant No. GK201603027 and No. GK201803019.

-
- [1] A. D. Sakharov, "Violation of CP Invariance, c Asymmetry, and Baryon Asymmetry of the Universe," *Pisma Zh. Eksp. Teor. Fiz.* **5** (1967) 32–35. [*Usp. Fiz. Nauk*161,61(1991)].
 - [2] **Planck** Collaboration, P. A. R. Ade *et al.*, "Planck 2013 results. XVI. Cosmological parameters," *Astron. Astrophys.* **571** (2014) A16, [arXiv:1303.5076 \[astro-ph.CO\]](#).
 - [3] E. Accomando *et al.*, "Workshop on CP Studies and Non-Standard Higgs Physics," [arXiv:hep-ph/0608079 \[hep-ph\]](#).
 - [4] D. E. Morrissey and M. J. Ramsey-Musolf, "Electroweak baryogenesis," *New J. Phys.* **14** (2012) 125003, [arXiv:1206.2942 \[hep-ph\]](#).
 - [5] Y. Gao, A. V. Gritsan, Z. Guo, K. Melnikov, M. Schulze, and N. V. Tran, "Spin determination of single-produced resonances at hadron colliders," *Phys. Rev.* **D81** (2010) 075022, [arXiv:1001.3396 \[hep-ph\]](#).
 - [6] S. Bolognesi, Y. Gao, A. V. Gritsan, K. Melnikov, M. Schulze, N. V. Tran, and A. Whitbeck, "On the spin and parity of a single-produced resonance at the LHC," *Phys. Rev.* **D86** (2012) 095031, [arXiv:1208.4018 \[hep-ph\]](#).
 - [7] A. V. Gritsan, R. Rentsch, M. Schulze, and M. Xiao, "Constraining anomalous Higgs boson couplings to the heavy flavor fermions using matrix element techniques," *Phys. Rev.* **D94** (2016) no. 5, 055023, [arXiv:1606.03107 \[hep-ph\]](#).
 - [8] J. Ellis and T. You, "Updated Global Analysis of Higgs Couplings," *JHEP* **06** (2013) 103, [arXiv:1303.3879 \[hep-ph\]](#).
 - [9] M. R. Buckley and D. Goncalves, "Boosting the Direct CP Measurement of the Higgs-Top Coupling," *Phys. Rev. Lett.* **116** (2016) no. 9, 091801, [arXiv:1507.07926 \[hep-ph\]](#).
 - [10] G. Li, H.-R. Wang, and S.-h. Zhu, "Probing CP-violating $h\bar{t}t$ coupling in $e^+e^- \rightarrow h\gamma$," *Phys. Rev.* **D93** (2016) no. 5, 055038, [arXiv:1506.06453 \[hep-ph\]](#).
 - [11] A. Hayreter, X.-G. He, and G. Valencia, "Yukawa sector for lepton flavor violating in $h \rightarrow \mu\tau$ and CP violation in $h \rightarrow \tau\tau$," *Phys. Rev.* **D94** (2016) no. 7, 075002, [arXiv:1606.00951 \[hep-ph\]](#).
 - [12] K. Hagiwara, K. Ma, and S. Mori, "Probing CP violation in $h \rightarrow \tau^-\tau^+$ at the LHC," *Phys. Rev. Lett.* **118** (2017) no. 17, 171802, [arXiv:1609.00943 \[hep-ph\]](#).
 - [13] M. J. Dolan, P. Harris, M. Jankowiak, and M. Spannowsky, "Constraining CP-violating Higgs Sectors at the LHC using gluon fusion," *Phys. Rev.* **D90** (2014) 073008, [arXiv:1406.3322 \[hep-ph\]](#).
 - [14] Y. Chen, A. Falkowski, I. Low, and R. Vega-Morales, "New Observables for CP Violation in Higgs Decays," *Phys. Rev.* **D90** (2014) no. 11, 113006, [arXiv:1405.6723 \[hep-ph\]](#).
 - [15] A. Yu. Korchin and V. A. Kovalchuk, "Angular distribution and forward/backward asymmetry of the Higgs-boson decay to photon and lepton pair," *Eur. Phys. J.* **C74** (2014) no. 11, 3141, [arXiv:1408.0342 \[hep-ph\]](#).
 - [16] X. Chen, G. Li, and X. Wan, "Probe CP violation in $H \rightarrow \gamma Z$ through forward-backward asymmetry," *Phys. Rev.* **D96** (2017) no. 5, 055023, [arXiv:1705.01254 \[hep-ph\]](#).
 - [17] L. Bian, N. Chen, and Y. Zhang, "CP violation effects in the diphoton spectrum of heavy scalars," *Phys. Rev.* **D96** (2017) no. 9, 095008, [arXiv:1706.09425 \[hep-ph\]](#).
 - [18] J. Brehmer, F. Kling, T. Plehn, and T. M. P. Tait, "Better Higgs-CP Tests Through Information Geometry," *Phys. Rev.* **D97** (2018) no. 9, 095017, [arXiv:1712.02350 \[hep-ph\]](#).
 - [19] **CMS** Collaboration, V. Khachatryan *et al.*, "Constraints on the spin-parity and anomalous HVV couplings of the Higgs boson in proton collisions at 7 and 8 TeV," *Phys. Rev.* **D92** (2015) no. 1, 012004, [arXiv:1411.3441 \[hep-ex\]](#).
 - [20] **CMS** Collaboration, V. Khachatryan *et al.*, "Combined search for anomalous pseudoscalar HVV couplings in $VH(H \rightarrow b\bar{b})$ production and $H \rightarrow VV$ decay," *Phys. Lett.* **B759** (2016) 672–696, [arXiv:1602.04305 \[hep-ex\]](#).
 - [21] **CMS** Collaboration, A. M. Sirunyan *et al.*, "Constraints on anomalous Higgs boson couplings using production and decay information in the four-lepton final state," *Phys. Lett.* **B775** (2017) 1–24,

- arXiv:1707.00541 [hep-ex].
- [22] **CMS** Collaboration, C. Collaboration, “Measurements of Higgs boson properties from on-shell and off-shell production in the four-lepton final state,”
 - [23] **ATLAS** Collaboration, G. Aad *et al.*, “Test of CP Invariance in vector-boson fusion production of the Higgs boson using the Optimal Observable method in the ditau decay channel with the ATLAS detector,” *Eur. Phys. J. C* **76** (2016) no. 12, 658, arXiv:1602.04516 [hep-ex].
 - [24] **ATLAS** Collaboration, M. Aaboud *et al.*, “Measurement of the Higgs boson coupling properties in the $H \rightarrow ZZ^* \rightarrow 4\ell$ decay channel at $\sqrt{s} = 13$ TeV with the ATLAS detector,” *JHEP* **03** (2018) 095, arXiv:1712.02304 [hep-ex].
 - [25] M. B. Voloshin, “CP Violation in Higgs Diphoton Decay in Models with Vectorlike Heavy Fermions,” *Phys. Rev. D* **86** (2012) 093016, arXiv:1208.4303 [hep-ph].
 - [26] F. Bishara, Y. Grossman, R. Harnik, D. J. Robinson, J. Shu, and J. Zupan, “Probing CP Violation in $h \rightarrow \gamma\gamma$ with Converted Photons,” *JHEP* **04** (2014) 084, arXiv:1312.2955 [hep-ph].
 - [27] Y. Chen, R. Harnik, and R. Vega-Morales, “Probing the Higgs Couplings to Photons in $h\gamma\gamma$ at the LHC,” *Phys. Rev. Lett.* **113** (2014) no. 19, 191801, arXiv:1404.1336 [hep-ph].
 - [28] D. A. Dicus and S. S. D. Willenbrock, “Photon Pair Production and the Intermediate Mass Higgs Boson,” *Phys. Rev. D* **37** (1988) 1801.
 - [29] L. J. Dixon and M. S. Siu, “Resonance continuum interference in the diphoton Higgs signal at the LHC,” *Phys. Rev. Lett.* **90** (2003) 252001, arXiv:hep-ph/0302233 [hep-ph].
 - [30] S. P. Martin, “Shift in the LHC Higgs diphoton mass peak from interference with background,” *Phys. Rev. D* **86** (2012) 073016, arXiv:1208.1533 [hep-ph].
 - [31] D. de Florian, N. Fianza, R. J. Hernandez-Pinto, J. Mazzitelli, Y. Rotstein Habarnau, and G. F. R. Sborlini, “A complete $O(\alpha_S^2)$ calculation of the signal-background interference for the Higgs diphoton decay channel,” *Eur. Phys. J. C* **73** (2013) no. 4, 2387, arXiv:1303.1397 [hep-ph].
 - [32] S. P. Martin, “Interference of Higgs diphoton signal and background in production with a jet at the LHC,” *Phys. Rev. D* **88** (2013) no. 1, 013004, arXiv:1303.3342 [hep-ph].
 - [33] L. J. Dixon and Y. Li, “Bounding the Higgs Boson Width Through Interferometry,” *Phys. Rev. Lett.* **111** (2013) 111802, arXiv:1305.3854 [hep-ph].
 - [34] J. Campbell, M. Carena, R. Harnik, and Z. Liu, “Interference in the $gg \rightarrow h \rightarrow \gamma\gamma$ On-Shell Rate and the Higgs Boson Total Width,” arXiv:1704.08259 [hep-ph].
 - [35] A. Djouadi, J. Ellis, and J. Quevillon, “Interference effects in the decays of spin-zero resonances into $\gamma\gamma$ and $t\bar{t}$,” *JHEP* **07** (2016) 105, arXiv:1605.00542 [hep-ph].
 - [36] B. Lillie, J. Shu, and T. M. P. Tait, “Kaluza-Klein Gluons as a Diagnostic of Warped Models,” *Phys. Rev. D* **76** (2007) 115016, arXiv:0706.3960 [hep-ph].
 - [37] L. Bian, D. Liu, J. Shu, and Y. Zhang, “Interference Effect on Resonance Studies in Searches of Heavy Particles,” *Int. J. Mod. Phys. B* **31** (2016) no. 14n15, 1650083, arXiv:1509.02787 [hep-ph].
 - [38] Z. Bern, A. De Freitas, and L. J. Dixon, “Two loop amplitudes for gluon fusion into two photons,” *JHEP* **09** (2001) 037, arXiv:hep-ph/0109078 [hep-ph].
 - [39] Z. Bern, L. J. Dixon, and C. Schmidt, “Isolating a light Higgs boson from the diphoton background at the CERN LHC,” *Phys. Rev. D* **66** (2002) 074018, arXiv:hep-ph/0206194 [hep-ph].
 - [40] J. M. Campbell, R. K. Ellis, and C. Williams, “Vector boson pair production at the LHC,” *JHEP* **07** (2011) 018, arXiv:1105.0020 [hep-ph].
 - [41] **CMS** Collaboration, C. Collaboration, “Measurements of properties of the Higgs boson in the diphoton decay channel with the full 2016 data set,” CMS-PAS-HIG-16-040.
 - [42] **ATLAS** Collaboration, M. Aaboud *et al.*, “Measurements of Higgs boson properties in the diphoton decay channel with 36 fb^{-1} of pp collision data at $\sqrt{s} = 13$ TeV with the ATLAS detector,” arXiv:1802.04146 [hep-ex].
 - [43] **ATLAS** Collaboration, ATLAS, “Projections for measurements of Higgs boson cross sections, branching ratios and coupling parameters with the ATLAS detector at a HL-LHC,” Tech. Rep. ATL-PHYS-PUB-2013-014, CERN, Geneva, Oct, 2013. <http://cds.cern.ch/record/1611186>.